

Displacement Self-sensing of Bearingless Switched Reluctance Motors Based on LS-SVM

Abstract. To achieve the rotor radial displacement self-sensing for a bearingless switched reluctance motor (BSRM), a new displacement estimation method using least squares support vector machine (LS-SVM) was proposed. Firstly, the working principle and mathematic of a 3-phase 12/8 pole BSRM was introduced in brief. Then taking advantage of LS-SVM with better solution for small-sample learning problem and strong generalization ability, two LS-SVMs were trained off-line to obtain two efficient nonlinear mapping structures to express the dynamic behavior of BSRM. The LS-SVM training data set is comprised of representative experimental data with current $\{i \mid i = (i_{sa1}, i_{sa2}, i_{ma})\}$ and rotor position θ as inputs and the corresponding displacements $\{D \mid D=(\alpha, \beta)\}$ as outputs. As well as giving a detailed explanation of the new method, simulation and experimental results were presented. It shows that the proposed LS-SVM-based displacement self-sensing method has high precision and operation efficiency.

Streszczenie. W artykule przedstawiono uczący się estymator przesunięcia dla bezłożyskowego silnika o przełączanej reluktancji (BSRM), wykorzystujący metodę LS-SVM (ang. Least Square Support Vector Machines). Opisano zasadę działania i model matematyczny silnika BSRM 3-fazowego 12/8 biegunowego. W celu uzyskania efektywnej struktury mapowania nieliniowego do określenia stanów dynamicznych, zastosowano dwa algorytmy, które zostały nauczone offline. Estymator poddano weryfikacji symulacyjnej i eksperymentalnej. (Zastosowanie metody LS-SVM w określaniu przemieszczenia w bezłożyskowym silniku o przełączanej reluktancji BSRM)

Keywords: Bearingless Motors; Switched Reluctance Motors; Least Squares Support Vector Machine; Self-sensing.

Słowa kluczowe: silniki bezłożyskowe, silniki o przełączanej reluktancji, LS-SVM.

Introduction

Bearingless switched reluctance motors (BSRMs) with simply doubly salient structure and combined characteristics of switched reluctance motors and magnetic bearings, makes it provide some unique features that suitable for running at high and super-high speed applications like flywheels. Many researchers are devoted to BSRMs' study [1-9], mainly on structure design [1], [2], electromagnetic analysis [3], [4], mathematics modeling [5], [6], and control strategy [7-9]. Recently, bearingless switched reluctance generators as a new hot topic is investigated in [10].

In BSRM system, rotor displacement must be measured to ensure the stable suspension. In practical magnetic suspending systems, displacement is often measured by eddycurrent sensors. Nevertheless, traditional sensors require periodic calibration and maintenance, sensitive to temperature and electro-magnetic noise, as well as tended to cause cost and complexity increment. As a result the reliability and the critical speed of BSRM are restricted. To eliminate the displacement sensors, several self-sensing methods for magnetic bearing systems have been reported [11-13]. The fundamental principle of self-sensing is the extraction of displacement information from circuit measurements or their derived parameters. Generally, the existing strategies may be divided into modulation [11], [12] and state observation [13]. However, due to the intrinsic nonlinearity and parameter uncertainty of BSRM, these strategies are difficult to get a satisfying solution.

Recently, artificial intelligence techniques have appeared in the literature for motion control [14-16], artificial neural network (ANN), as a kind of intelligent control method, can get rid of the dependence of control object and obtain a better treatable and robustness in dealing with the problem of nonlinear and uncertainty. In [15], [16], ANN is used in switched reluctance motor (SRM) closed-loop system as a position and speed estimator. However, when ANN is used, some drawbacks can be mentioned: 1) a great amount of training samples in training, 2) the selection of network topology and the determination of initial weighted value is mainly according to experience, 3) problems of local minimum and over-fitting. These shortcomings are always the difficult problems of ANN in application. Compared to ANN, support vector machines (SVM), as a new machine learning method proposed by V. Vapnik [17], has been

widely used in nonlinear modeling and control areas in recent years. The training process of SVM follows structural risk minimization principle and small sample study has strong generalization ability. Its structure and parameters are formed automatically in the training process by the samples. And least squares support vector machine (LS-SVM), proposed by J. A. K. Suykens [18], defines a cost function which is different from classical SVM and changes its inequation restriction to equation restriction, which greatly accelerates the solution speed and there is no local minimum question. Therefore the LS-SVM can successfully overcome the defects of ANN, and have better performance and wider application. In [19], an approach of rotor position estimation for SRM based on SVM is presented. In [20], [21], LS-SVM is used to estimate the rotor displacement for magnetic bearings and to identify the inverse model for BSRM decoupling control.

This paper presents a rotor displacement self-sensing approach for a 3-phase 12/8 pole BSRM. The basic premise of the method is that two different LS-SVMs are trained off-line to form two very efficient mapping structures for α - and β -direction displacement system of BSRM respectively. Through the measurement of currents $\{i \mid i = (i_{sa1}, i_{sa2}, i_{ma})\}$ and rotor position (θ), two LS-SVMs are able to estimate the rotor displacements $\{D \mid D=(\alpha, \beta)\}$, thereby facilitating elimination of the rotor displacement sensors.

Modeling of 3-phase 12/8-pole BSRM

Fig.1(a) shows the windings configuration of a 3-phase 12/8-pole BSRM. There are 4-pole motor windings and 2-pole suspension windings in one stator. The 4-pole motor windings are placed outside in the stator slots. The inside conductors are for the 2-pole radial suspension force windings. Fig.1(b) shows the principle of radial force production, only A-phase windings are shown. ψ_{ma} is the 4-pole fluxes produced by the 4-pole motor windings current i_{ma} . If the rotor is placed at the center of the motor, the flux densities at the poles are equal to each other. At this time, if the 2-pole flux ψ_{sa1} is generated by the 2-pole suspension windings N_{sa1} , the flux density increases at the air-gap1, and decreases at the air-gap2. The symmetrical 4-pole flux distribution is unbalanced, This unbalanced flux distribution results in radial force F_{α} , which is exerted in the α -axis positive direction, as shown in Fig.1(b). A radial force in the

α axis negative direction can be produced with a negative current in N_{sa1} . Besides, a radial force F_β in the β axis can be produced by the 2-pole suspension winding N_{sa2} . Thus, radial force can be produced in any desired direction. Similarly, this principle can be applied to the B- and C-phases. And the radial force can be generated continuously by these three phases for every 15° .

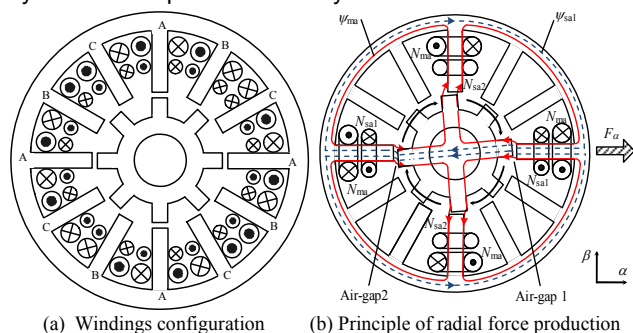


Fig.1. Windings configuration and principle of radial force

The theoretical formulas of instantaneous radial forces of the A-phase can be developed from the inductance matrix based on the simple magnetic equivalent circuit. Under some general assumptions, such as neglecting the leakage flux and saturation effects, the mathematical model of the instantaneous radial forces F_α and F_β , consider the cross coupling between the α - and β -direction radial forces, are derived from the derivatives of the stored magnetic energy W based on the inductance matrix with respect to the α - and β -direction displacements α and β , respectively, $F_\alpha = \partial W / \partial \alpha$, $F_\beta = \partial W / \partial \beta$. The theoretical formulas of instantaneous radial forces of the A-phase are written in matrix form from [14] as

$$(1) \quad \begin{bmatrix} F_\alpha \\ F_\beta \end{bmatrix} = i_{ma} \begin{bmatrix} k_1(\theta) & -k_2(\theta) \\ k_2(\theta) & k_1(\theta) \end{bmatrix} \begin{bmatrix} i_{sa1} \\ i_{sa2} \end{bmatrix}$$

Where, i_{ma} , i_{sa1} and i_{sa2} are the instantaneous currents in A-phase 4-pole motor main windings N_{ma} and 2-pole radial force windings N_{sa1} and N_{sa2} , respectively; $k_1(\theta)$ and $k_2(\theta)$ are the function of the rotor angular position θ and the dimensions of the test motor. When the configuration of test motor is fixed, $k_1(\theta)$ and $k_2(\theta)$ are only related to angular position θ . In this paper, the calculate formulas of $k_1(\theta)$ and $k_2(\theta)$ is skipped. Interested readers are referred to [14] for detailed information.

Furthermore, neglecting the external interfere forces, the motion equation of magnetic suspension rotor can be written as

$$(2) \quad F_\alpha = m\ddot{\alpha}, F_\beta = m\ddot{\beta} + mg$$

Hence, the α - and β -direction displacements α and β can be obtained from (1) and (2) as the following form:

$$(3) \quad \begin{bmatrix} \alpha \\ \beta \end{bmatrix} = \iint \left\{ \frac{1}{m} \begin{bmatrix} F_\alpha \\ F_\beta \end{bmatrix} + \begin{bmatrix} 0 \\ -g \end{bmatrix} \right\} + \begin{bmatrix} \alpha_0 \\ \beta_0 \end{bmatrix}$$

Note that α_0 and β_0 are equal to zero, since the rotor is almost time suspending at the center point of motor. So (3) can be then rewritten as

$$(4) \quad \begin{bmatrix} \alpha \\ \beta \end{bmatrix} = \iint \left\{ \frac{i_{ma}}{m} \begin{bmatrix} k_1(\theta) & -k_2(\theta) \\ k_2(\theta) & k_1(\theta) \end{bmatrix} \begin{bmatrix} i_{sa1} \\ i_{sa2} \end{bmatrix} + \begin{bmatrix} 0 \\ -g \end{bmatrix} \right\}$$

From the equ.4, we can see that the rotor displacements α and β are related to the currents $\{i \mid i = (i_{sa1}, i_{sa2}, i_{ma})\}$ and the

position θ . So through the measurement of the currents $\{i \mid i = (i_{sa1}, i_{sa2}, i_{ma})\}$ and the position (θ), the rotor displacements $\{D \mid D = (\alpha, \beta)\}$ can be estimated by equ.4. But due to the intrinsic nonlinearity and parameter uncertainty of BSRM, equ.4 cannot express the accurately relationship among i , θ and D when the BSRM operates in different state. Hence, to overcome the drawbacks of the analytical model equ.4, this paper takes advantage of LS-SVM with better solution for small-sample learning problem and good generalization ability to identify the relationship among i , θ and D .

Least squares support vector machine

Consider a given set of training samples $\{x_k, y_k\}_{k=1,2,\dots,N}$, where x_k is the input vector and y_k is the corresponding target value for sample k . With a LS-SVM, the relation underlying the data set is represented as a function of the following form:

$$(5) \quad \hat{y}(x) = w^T \varphi(x) + b.$$

Where φ is a mapping of the vector x to some (probably high-dimensional) feature space, b is the bias and w is a weight vector of the same dimension as the feature space. For the LS-SVM regression, we introduce error variables for the fitting problem as follows:

$$(6) \quad e_k = w^T \varphi(x) + b - y_k.$$

and for the given data we search for those weights that give the smallest summed quadratic error of the training samples in case of LS-SVM. Because this can easily lead to over-fitting, ridge regression (a form of regularization) is used to smoothen the approximation. The minimization of the error together with the regularization is given as

$$(7) \quad \min J(w, e) = \frac{1}{2} w^T w + \frac{\gamma}{2} \sum_{k=1}^N e_k^2$$

$$(8) \quad \text{s.t. } y_k = w^T \varphi(x_k) + b + e_k, k = 1, 2, \dots, L.$$

where γ is the regularization parameter.

This problem can be solved using optimization theory. Instead of minimizing the primary objective (7), a dual objective, the so-called Lagrangian, can be formed of which the saddle point is the optimum. The Lagrangian for this problem is given as:

$$(9) \quad L(w, a, b, e) = J + \sum_{k=1}^L a_k [y_k - w^T \varphi(x_k) - b - e_k].$$

Where a_k is called the Lagrangian multiplier.

With Karush-Kuhn-Tucker conditions, the solution is given by the following set of linear equations:

$$(10) \quad \begin{bmatrix} 0 & \mathbf{I}^T \\ \mathbf{I} & \mathbf{K} + \gamma^{-1} \mathbf{I} \end{bmatrix} \begin{bmatrix} b \\ \alpha \end{bmatrix} = \begin{bmatrix} 0 \\ \mathbf{y} \end{bmatrix}.$$

Where α is the L -vector $\alpha = [\alpha_1, \dots, \alpha_L]^T$, \mathbf{y} is the corresponding vector of y_k -values $\mathbf{y} = [y_1, \dots, y_L]^T$, \mathbf{I} is the unity L -vector, and \mathbf{K} is the $L \times L$ 'Kernel matrix'. The elements of matrix \mathbf{K} equal $K_{ij} = \varphi(x_i)^T \varphi(x_j) = K(x_i, x_j)$, $i, j = 1, 2, \dots, L$. $K(x_i, x_j)$ is symmetric function which satisfies Mercer condition. Kernel function is often used result in an approximation by radial basis function (RBF), by polynomial functions, or by splines. In this paper we focus on the RBF kernel:

$$(11) \quad K(x_i, x_j) = \exp[-|x_i - x_j|^2 / (2\sigma^2)].$$

The solution of the set of equations (6) results in a vector of Lagrangian multipliers α and a bias b . The output of the approximator can be calculated for new input values of x , with α and b . The output is given as

$$(12) \quad \hat{y}(x) = \sum_{k=1}^L \alpha_k K(x_k, x) + b.$$

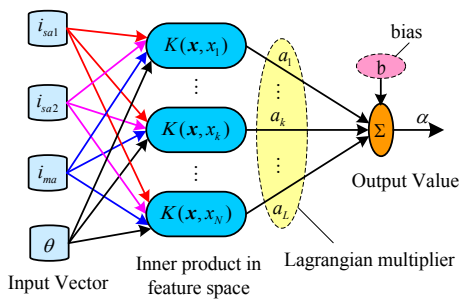


Fig.2 The mapping structure of LS-SVM α

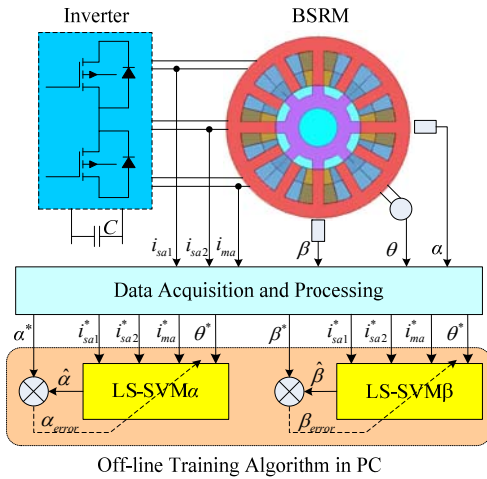


Fig.3 Data collecting and two LS-SVMs off-line training

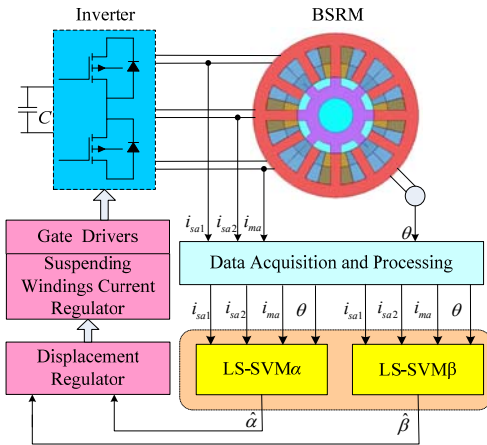


Fig.4 LS-SVM-based displacements self-sensing

LS-SVM-based displacement self-sensing for 3-phase 12/8-pole BSRM

The basic premise of the proposed LS-SVM-based rotor displacement self-sensing method is that two different LS-SVMs are trained off-line to form two very efficient mapping structures for α - and β -direction displacement system of BSRM respectively. Through the measurement of currents $\{i \mid i = (i_{sa1}, i_{sa2}, i_{ma})\}$ and rotor position θ , two LS-SVMs are able to estimate the rotor displacements $\{D \mid D = (\alpha, \beta)\}$, thereby facilitating elimination of the rotor displacement sensors. Fig.2 shows the mapping structure of α -direction displacement model, LS-SVM α . the β -direction displacement mapping structure is similar to LS-SVM α , it is named LS-SVM β . LS-SVMs training data is comprised of currents

i and position θ serve as inputs and displacement D as output. Given a representatively training data set, two different LS-SVMs can identify the correlation among i , θ and D . Then the two trained LS-SVM can be evaluated against a test data set which have different values.

Initially, the data obtained from FEA were used to train the two LS-SVMs. but the experimental implementation of LS-SVMs after training showed considerable error in the rotor displacements estimate. Sampling error and noise introduced during analogue-to-digital conversion processes in the experimental system result in erroneous estimation of the rotor displacements. As a result, the experimental data, which are representatives of physical phenomena, have to be constructed. Therefore, the experimental system is executed in the displacement sensed mode. The two LS-SVMs that would be off-line trained by this experimentally captured data would negate the effects of noise, sampling, and estimation errors. Experimental data are collected in closed loop control system. A total of 2000 data points is randomly selected from the captured magnetization characteristics and used for training. Fig.3 shows how experimental data was collected and how two LS-SVMs are trained off-line.

Experimental results

To verify the effectiveness of the proposed method, the displacement self-sensing for 3-Phase 12/8-Pole BSRM is conducted. The system block used in the experiment is shown in Fig.4. The parameters of prototype are listed in Tab.1. And the experimental results are presented here.

Tab.1 Parameters of prototype

parameters	value	parameters	value
N_{ma} /[turns]	60	m /[kg]	1
N_{sa} /[turns]	24	h /[m]	0.1
l_g /[m]	3×10^{-4}	J /[kg·m ²]	9×10^{-3}
l_o /[m]	2.5×10^{-4}	N_{i_r} /[H/A]	$4\pi \times 10^{-7}$

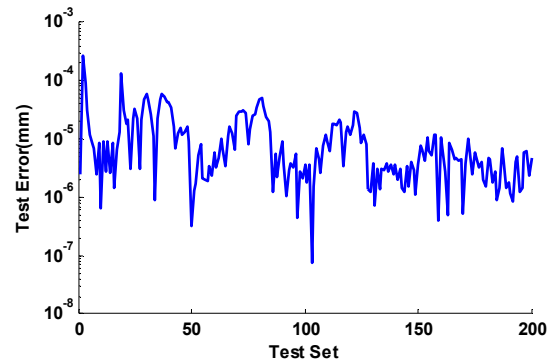


Fig.5 LS-SVM Generalization performance

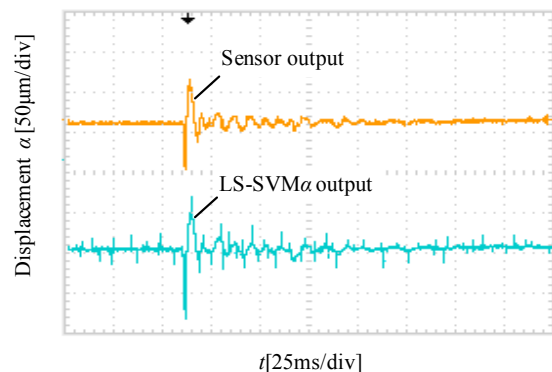


Fig.6. measured displacement and estimated displacement

Shown in Figure 5 is the test error of LS-SVM α at 200 test data points that are not part of the training set in experimentally captured data. This is done to analyze the generalization capability of LS-SVM, From the error curve we can see that the test error is small, and the max value is 0.1 μ m, it is much less than the average air gap 0.3mm. So the LS-SVM α has a strong generalization performance.

Figure 6 shows the comparison of the estimated rotor displacement $\hat{\alpha}$ and the eddy-current sensor output α . The reference of the rotor displacement is intentionally changed with a shock wave. It is seen that the estimated rotor displacement includes a certain level of noises. However, a good correspondence is seen with the proxy sensor. Therefore, it is shown that the proposed self-sensing method of the rotor displacement is quite effective.

Conclusions

The work presented in this paper describes a LS-SVM-based displacement self-sensing method for a BSRM. The approach is to train two LS-SVMs to estimate rotor displacement for given phase current and rotor position. Two effective mapping structures were obtained through two LS-SVMs off-line training by the experimental data. The simulation and experimental results verify the effectiveness of the proposed method.

Acknowledgments

This work was supported by National Natural Science Foundation of China (Grant No. 61074019) and Program granted for scientific innovation research of college graduate in Jiangsu province (Grant No. CXZZ12_0686).

REFERENCES

- [1] L. Chen, W. Hofmann. Speed regulation technique of bearingless 8/6 switched reluctance motor with simpler single winding structure, IEEE Trans. Ind. Electron., 59(2012):2592-2600.
- [2] F. C. Lin, S. M. Yang. Self-Bearing Control of a switched reluctance motor using sinusoidal currents, IEEE Trans. Power Electron., 22(2007): 2518 -2526.
- [3] C. R. Morrison, M. W. Siebert, E. J. Ho. Electromagnetic forces in a hybrid magnetic-bearing switched-reluctance motor, IEEE Trans. Magn.,44(2008): 4626–4638.
- [4] M. Takemoto, A. Chiba, H. Akagi. Radial force and torque of a bearingless switched reluctance motor operating in a region of magnetic saturation, IEEE Trans. Ind. App., 40(2004): 103–112.
- [5] X. Cao, Z. Deng, G. Yang, Y. Yang. Mathematical model of bearingless switched reluctance motors based on maxwell stress tensor method, Proceedings of the CSEE, 29(2009): 78–83.
- [6] Y. Sun, J Wu, Q. Xiang, The mathematic model of bearingless switched reluctance motor based on the finite-element analysis, Proceedings of the CSEE, 27(2007): 33-40.
- [7] M. Takemoto, A. Chiba, T. Fukao. A method of determining

- the advanced angle of square-wave currents in bearingless switched reluctance motor, IEEE Trans. Ind. Appl., 37 (2001):1702–1709.
- [8] X. Cao, Z. Deng, G. Yang, X. Wang, Independent control of average torque and radial force in bearingless switched-reluctance motors with hybrid excitations, IEEE Trans. Power Electron., 24(2009): 1376–1385.
 - [9] Y. Yang, Z. Deng, G. Yang, X. Cao. A control strategy for bearingless switched-reluctance motors, IEEE Trans. Power Electron., 25(2010):2807-2819.
 - [10] X. Cao, Z. Deng. A full-period generating mode for bearingless switched reluctance generators, IEEE Trans. Appl. Supercond., 20(2010):1072-1076.
 - [11] T. Kuwajima, T. Nobe, K. Ebara, A. Chiba, and T. Fukao, An estimation of the rotor displacements of bearingless motors based on a high frequency equivalent circuits, Proc. IEEE Power Electro. Drive Syst., 2(2001):725-731.
 - [12] T. Tera, Y. Yamauchi, A. Chiba. Performances of bearingless and sensorless induction motor drive based on mutual inductances and rotor displacements estimation, IEEE Trans. Power Electron, 53(2006):187-194.
 - [13] T. Mizuno, K. Araki, H. Bleuler. Stability analysis of self-sensing magnetic bearing controllers, IEEE Trans. Contr. Syst. Technol., 4(1996): 572-579.
 - [14] Y. Sun, Y. Zhou, X. Ji. Decoupling control of bearingless switched reluctance motor with neural network inverse system method, Proceeding of the CSEE, 31(2011): 117-123.
 - [15] C. A. Hudson, N. S. Lobo, R. Krishnan. Sensorless control of single switch-based switched reluctance motor drive using neural network, IEEE Trans. Ind. Electron,55(2008):321 - 329.
 - [16] E. Mese and D. A. Torrey, An approach for sensorless position estimation for switched reluctance motors using artificial neural networks, IEEE Trans. Ind. Electron, 17(2002): 66-75.
 - [17] V. Vapnik. New York: Springer-Verlag, (1999).
 - [18] J. A. K. Snykens, European Journal of Control, 7(2001).
 - [19] C. Xia, Z. He, Y. Zhou, X. Xie. Rotor position estimation for switched reluctance motors based on support vector machine Trans. China electro-technical Society, 22(2007):12-17.
 - [20] Z. Zhu, Y. Sun. Rotor displacement estimation for MB sensorless control, Przegląd Elektrotechniczny, 88(2012):141-145.
 - [21] Z. Zhu, Y. Sun, Y. Huang. Inverse dynamics modeling and control for bearingless switched reluctance motor, Electric Mach. and Contr., 15(2011):74-79.

Authors: dr Zhiying ZHU, School of Electrical and Information Engineering, Jiangsu University, Zhenjiang 212013 China, E-mail: ujszzy@gmail.com; prof. Yukun SUN, intelligent control of special motors, Nanjing Institute of Technology, Nanjing 210013 China, E-mail: syk@ujts.edu.cn; Prof. Yonghong Huang, School of Electrical and Information Engineering, Jiangsu University, Zhenjiang 212013 China, hyh@ujts.edu.cn; Asso. Prof. Xiaofu Ji, robust control and filtering, descriptor systems, and time delay systems, School of Electrical and Information Engineering, Jiangsu University, Zhenjiang 212013 China, xji@sina.com.